PROCEEDINGS OF SPIE

SPIEDigitalLibrary.org/conference-proceedings-of-spie

Optical instrument design of the high-energy x-ray probe (HEX-P)

Kristin K. Madsen, Fiona Harrison, D. Broadway, F. E. Christensen, M. Descalle, et al.

Kristin K. Madsen, Fiona Harrison, D. Broadway, F. E. Christensen, M. Descalle, D. Ferreira, B. Grefenstette, D. Gurgew, A. Hornschemeier, H. Miyasaka, T. Okajima, S. Pike, M. Pivovaroff, T. Saha, D. Stern, J. Vogel, D. Windt, W. Zhang, "Optical instrument design of the high-energy x-ray probe (HEX-P)," Proc. SPIE 10699, Space Telescopes and Instrumentation 2018: Ultraviolet to Gamma Ray, 106996M (6 July 2018); doi: 10.1117/12.2314117

SPIE.

Event: SPIE Astronomical Telescopes + Instrumentation, 2018, Austin, Texas, United States

Optical instrument design of the High-Energy X-ray Probe (HEX-P)

Kristin K. Madsen[a], Fiona A. Harrison[a], D. Broadway[b], F. E. Christensen[c], M. Descalle[d], D. Ferreira[c], B. Grefenstette[a], D. Gurgew[e], A. Hornschemeier[f], H. Miyasaka[a], T. Okajima[f], S. Pike[a], M. Pivovaroff[d], T. Saha[f], D. Stern[g], J. Vogel[d], D. Windt[h], and W. Zhang[f]

[a]California Institute of Technology, Pasadena, USA
[b]NASA Marshall Space Flight Center, Huntsville, USA
[c]DTU Space, Lyngby, Denmark
[d]Lawrence Livermore National Laboratory, Livermore, CA, USA
[e]University of Alabama, Huntsville, USA
[f]NASA Goddard Space Flight Center, Greenbelt, USA
[g]Jet Propulsion Laboratory, California Institute of Technology, Pasadena, CA 91109, USA
[h]Reflective X-ray Optics, New York, USA

ABSTRACT

The *High-Energy X-ray Probe* (*HEX-P*) is a probe-class next-generation high-energy X-ray mission concept that will vastly extend the reach of broadband X-ray observations. Studying the 2-200 keV energy range, *HEX-P* has 40 times the sensitivity of any previous mission in the 10-80 keV band, and will be the first focusing instrument in the 80-200 keV band. A successor to the *Nuclear Spectroscopic Telescope Array* (*NuSTAR*), a NASA Small Explorer launched in 2012, *HEX-P* addresses key NASA science objectives, and will serve as an important complement to ESA's L-class *Athena* mission. *HEX-P* will utilize multilayer coated X-ray optics, and in this paper we present the details of the optical design, and discuss the multilayer prescriptions necessary for the reflection of hard X-ray photons. We consider multiple module designs with the aim of investigating the tradeoff between high- and low-energy effective area, and review the technology development necessary to reach that goal within the next decade.

Keywords: HEX-P, X-ray, Satellite

1. HEX-P MISSION CONCEPT OVERVIEW

The *Nuclear Spectroscopic Telescope Array* (*NuSTAR*)[1] Small Explorer opened the high-energy (> 10 keV) X-ray band and established the power of broad-band X-ray spectroscopy for probing the Universe, from regions near accreting black holes to the diffuse remnants of exploded stars. *HEX-P* (see paper no. 10699-82 in these proceedings) is a probe-class concept (cost bracket \$500M-1B) that will expand the focused X-ray band up to 200 keV from the previous 80 keV limit of *NuSTAR*.

HEX-P is envisioned as a general purpose observatory with focusing Wolter-I X-ray optics operating in the 2-200 keV band. To achieve such energies, the focal length is 20 m, necessitating an extendible mast and multilayer coated lightweight mirrors. *HEX-P* is baselined for an angular resolution with a half power diameter (HPD) of $15''$, considered a feasible target within the next decade.[2] *HEX-P* will have three modules composed of $\sim$270 nested shells focusing onto individual detectors, and building on the *NuSTAR* heritage, *HEX-P* will employ CdTe photon counting detectors with a spectral resolution of 200 eV at 6 keV and 800 eV at 60 keV. These detectors will be countrate-limited at 10 kHz (25 times the *NuSTAR* rate) and offer a timing resolution of 1μs. Compared to *NuSTAR* *HEX-P* will have $\sim$40 times increased sensitivity to faint sources and 25 times higher throughput for bright sources.

Further author information: (Send correspondence to K.K.M.)
K.K.M.: E-mail: kristin@srl.caltech.edu, phone: +1 626 395 6634

Space Telescopes and Instrumentation 2018: Ultraviolet to Gamma Ray, edited by Jan-Willem A. den Herder, Shouleh Nikzad, Kazuhiro Nakazawa, Proc. of SPIE Vol. 10699, 106996M · © 2018 SPIE
CCC code: 0277-786X/18/$18 · doi: 10.1117/12.2314117

Table 1. Instrument Baseline Design Parameters

Specifications	
Focal length	20,000 mm
Inner radius	50 mm
Outer radius	350 mm
Incident angle range	0.6 - 4.3 mrad
Shell length	300 mm
Substrate thickness	0.25 mm
Number of shells	276
Shell spacing [a]	1.33
Reflective coating	Section 3

[a] Multiple of 'close packed' spacing.

With this leap in observational capability, *HEX-P* will address a broad range of science objective, from probing the extreme environments around black holes and neutron stars, to mapping the growth of supermassive black holes and the effect they have on their environments. If developed and launched on a timescale similar to *Athena*, *HEX-P* would support simultaneous observations, greatly enhancing the ability of *Athena* to probe a range of phenomena where sensitivity above 10 keV is essential to interpreting their spectra.

2. INSTRUMENT DESIGN

To enable the reflection of 200 keV photons, shallow graze angles are required. A fair approximation for how small can be made by considering the Bragg condition $\lambda m = 2dsin\theta_i$, where d is the lattice spacing of a crystal or multilayer coating, m the Bragg order, and θ_i the incidence angle, and λ the wavelength. Smaller lattice spacings reflect harder energies, and if we adopt a value of 3 nm for the d-spacing, which is an achievable value for many periodic material coatings, then for the 1st order Bragg peak the required incidence angle is 1 mrad. The smallest graze angle of *NuSTAR* (focal length 10 m) is 1.3 mrad at a radius of 54 mm, and since it is difficult to make mirrors with radius of curvature less than 50 mm, a focal length of greater than 10 m will be required. For Wolter-I optics the relation between focal length, F, and radius, r, is given by $r = 4\alpha F$, and a graze angle of α =1 mrad requires at least a focal length of 12.5 m. This would, of course, only barely get the job done, as at least a number of mirror shells should be able to reflect 200 keV photons to have an appreciable effective area. For *HEX-P* we have therefore chosen 20 m as the baseline.

Extending the focal length beyond 20 m becomes challenging from a focal plane point of view, since the platescale of the focal will grow as the square of the focal length. At 20 m obtaining a field of view (FoV) of $12'$, comparable to *NuSTAR*, with *NuSTAR* sized detectors, will require a detector array of 4×4 crystals. The placescale will be 10.3 arcsec mm^{-1}, and a PSF with an HPD of $15''$ will be contained inside a diameter of 1.5 mm. To adequately sample the HPD the design requirement on the detector pitch has been set to 300μm, well achievable with current technologies (see paper no. 10699-202 in this proceedings).

Table 1 lists the baseline parameters. As noted above, the inner radius at 50 mm is the current practical limit for mirror curvature for both segmented glass and full shells of revolution. A similar argument holds for the outer radius at 350 mm. Section 3 discusses the multilayer considerations.

2.1 Detailed Instrument Design

Maximizing the geometric area is not as straightforward as it may seem. The highest possible achievable geometric area would be obtained if the aperture between inner and outer radius could be entirely filled without any obstruction. That is not possible due to the finite width of the nested mirror shells, and in this case the ideal packing with respect to the maximum geometric area, is by aligning the shells such that the lower front edge of the upper parabolic mirror, when starting from the outside, is aligned with the backside of the adjacent shell. This is often called 'close packing' and maximizes the on-axis geometrical area. However, it results in obscuration from neighboring shells when moving off-axis, and the solution is to allow for extra shell-spacing to increase the

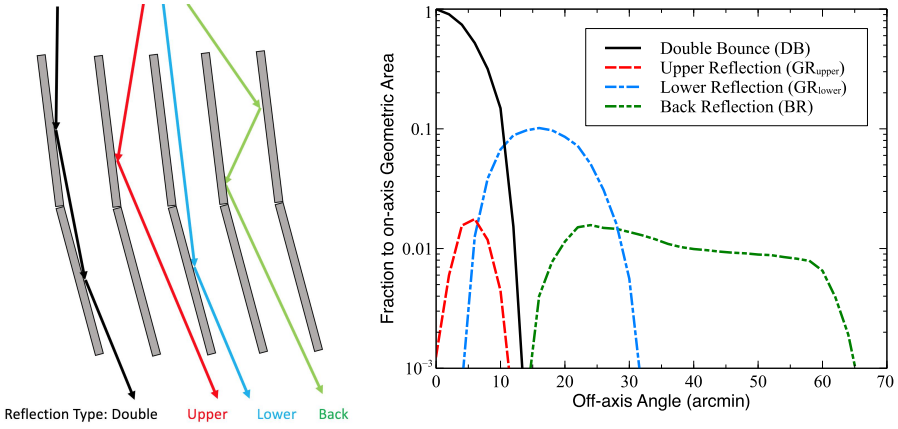

Figure 1. **Left**: Illustration of different types of reflection in the optics. Black is the nominal double bounced reflection, which focuses the photons onto the focal plane. Red and blue are single reflection of the upper and lower conical mirror sections, collectively termed Ghost Rays (GR). The green ray illustrates the back reflection (BR) situation where a photon strikes the backside of the adjacent mirror, then reflects off the front side of the upper section and exits the optics. **Right**: The relative geometric area of the various components with respect to the on-axis geometric area. The areas have been corrected for the finite detector size.

off-axis area. This, unfortunately, allows photons, which are reflected only once (see Figure 1), either by the top or bottom mirror, to reach the focal plane. These single-bounce photons, sometimes referred to as ghost-rays (GR), leave very distinct features on the focal plane, which can interfere with the properly focused PSF, and are, from a scientific point of view, undesirable.

Balancing the on- and off-axis geometrical area against the single-bounce photons can be a difficult task, and though analytical tools exist to assist in the estimation[3–5] there is no clear metric for the best solution, since some amount of GR is unavoidable, and it remains a decision that is unique to each optic and its particular use. Evaluating the analytical expressions and drawing on our experience with *NuSTAR*, we decided to stay with the same shell packing that we had for *NuSTAR*, which has a shell spacing of 4/3 × the 'close packing' spacing. Figure 1 shows the relative intensities of the non-focused components of the baseline, which have taken into account the finite detector size. The single bounce components die out at around 10″, while the back-reflected component extends up to 65″. These values are for all the GR photons collected on the detector, but the pattern of the GR is very structured and the actual source to GR fraction is greatly dependent on position on the detector. We have found that most cases of GR contamination in *NuSTAR* can be mitigated by careful positioning of the source.[6] Baffling can be employed to reduce the remaining component further, and we will be studying possible designs.

Once the inner and outer radii are set, the third parameter that can be used to adjust the area is the shell length. To investigate the phase space around our baseline, we calculated the geometric area and mass as a function of shell length and shell thickness, assuming for the substrate the density of Si. Figure 2 shows the number of shells, geometric area, and mass as a function of shell length. This demonstrates that there is significant area to be gained by increasing the shell length. Though this results in fewer shells, there is still a net increase in mass. A 10 mm increase in shell length results in an approximate gain of 5-8% in area, but with comparable increase in mass. The mass to shell length increase is roughly linear at a fixed shell thickness, but the efficiency of area to mass is a decreasing function of shell thickness, T, and can be approximated as: (area/mass)$=40 - 40.5 \times T$(mm). None of this is surprising, but important from a production point of view since longer shells significantly reduce the required number of shells, which may become very important for the mounting of the shells. Independent of the size and number of shells, some mounting fixturing will be required and may be a significant source of obscuration, in which case fewer shells of longer length could become favorable. With the current baseline, each optic has a pure glass mass of ∼120 kg, with a geometric area of ∼2300 cm^2.

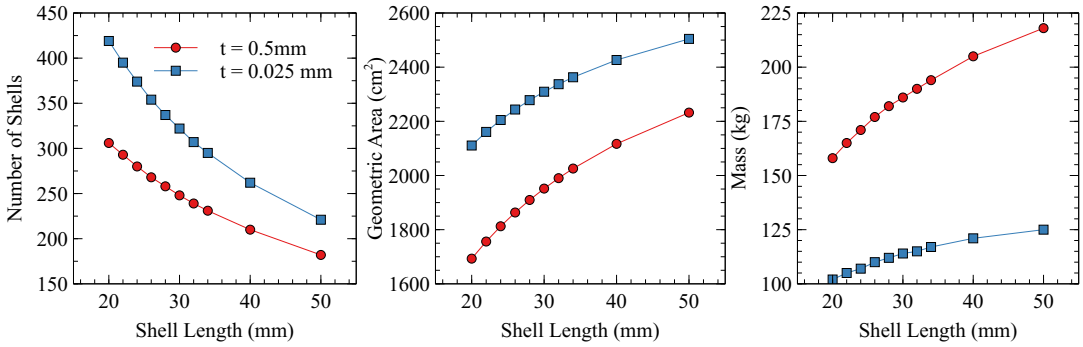

Figure 2. Shell length as functions of number of shells, area, and mass for shell thickness of 0.025 mm (blue; square) and 0.05 mm (red; circle).

3. MULTILAYER DESIGN

3.1 Depth-graded Multilayers

Multilayers have long been in use for UV lithography, neutron beam lines and in laboratory X-ray systems to focus and shape beams. However, it is only in the last two decades that these principles have been applied to astrophysical optics. A multilayer is a stack of thinly deposited films of alternating materials, where one set of high-Z and low-Z film is called a bi-layer. The thickness of the individual films determines the shape of the spectrum. For example, a constant thickness of the bi-layer will result in a spectrum with a good response at a few monochromatic energies, at the location of the Bragg peak, but otherwise have a poor broadband spectral response. Far more convenient is a power-law graded stack,[7] which through a varying bi-layer thickness ensures that the Bragg peaks are shifted through the spectrum, providing a broadband response. The bi-layer thickness, d_i, of the power-law stack is defined by

$$d_i = \frac{a}{(b+i)^c} \qquad i = 1, N \tag{1}$$

where N is the number of bi-layers in the stack. The bi-layer i=1 is the top and thickest bi-layer. The fraction of the high-density material to the thickness of the bi-layer is given by $\Gamma = d_{\mathrm{highZ}}/d$, and once c is chosen then the maximum and minimum d-spacing, d_{max}, d_{min}, determine parameters a and b. The power law index c controls the relative shifts of the Bragg peaks; a low c drives them apart, while a high c drives them together. Combined with the choice of material, these five parameters define the multilayer.

A power-law graded profile was used for the *High-Energy Forcusing Telescope* (*HEFT*),[8] which was a balloon mission flown in 2005. For *NuSTAR* we added a sixth parameter, Γ_{top}, which is the relative thickness of the heavy material to the bi-layer thickness of the first layer at the top of the stack. This parameter ensures that the dense material is thick enough in the top layer to ensure proper total external reflection from angles below the critical angle.[9]

Another successfully applied depth-graded structure is the block-method employed by *InFOCuS*[10] and *Hitomi*.[11] In this structure, rather than continuously changing the thickness of the bi-layers down through the stack, it contains blocks of bi-layers with periodic constant spacing. The principle is the same as for the power-law depth-graded profile in which by changing the bi-layer thickness, the Bragg peaks are shifted through the spectrum. But rather than a continuous shifting achieved by each layer, the block shifts are discrete with several layers contributing to one Bragg peak. The power-law and block method tend to yield similar responses when optimized to the same telescope design.

while we plan future investigations of different depth-graded profiles, here we only discuss the power-law depth-graded profile, for which we have an optimization routine.

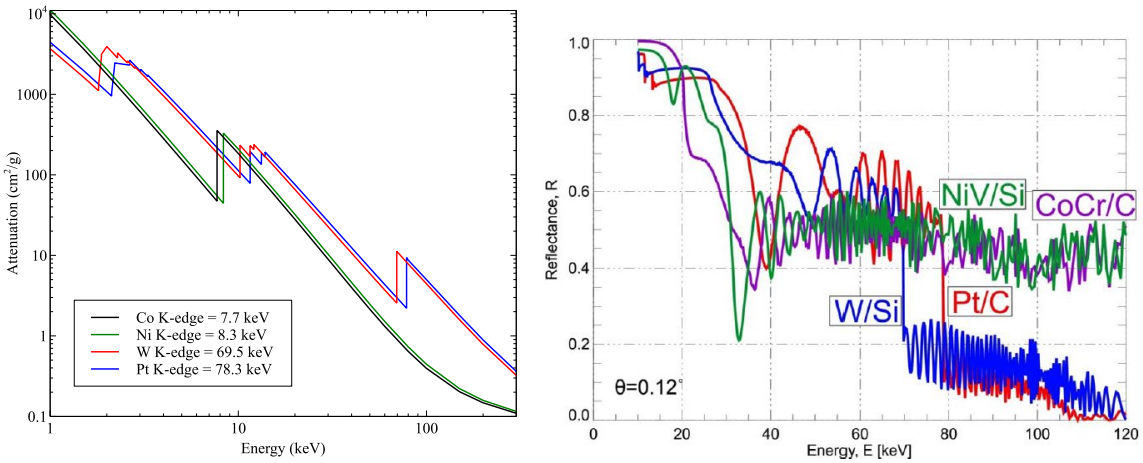

Figure 3. **Left:** Attenuation curves of Co, Ni, W, and Pt. **Right:** Theoretical performances of optimized depth-graded multilayers for the respective material combinations (Credit:[16]).

3.2 Material Selection

The typical families considered for hard X-ray astrophysical applications are Co-, Ni-, W-, and Pt-based coatings. Because Pt has the highest energy K-edge (78.3 keV), and thus the broadest bandpass, Pt/C was favored by *NuSTAR* and *Hitomi*. However, the W-based family has both better interfacial roughness and can be deposited more thinly, and for this reason *NuSTAR* included both Pt/C and W/Si in its design, applying Pt/C only on mirrors that contributed to area between 70–80 keV. W-based coatings have long been suggested as reflectors for energies above 100 keV[12–16] and been measured at energies above 80 keV, demonstrating that their performance matches the theoretical predictions at those energies.[12,13,16] Pt has not been as well-studied at high energies, primarily because of the cost of obtaining a target, and depending on the achievable interface widths, which have yet to be investigated, Pt-based multilayers may allow performance comparable to, or potentially even better than W-based coatings.

For astrophysical applications, a broad bandpass is desirable since objects typically emit across a wide spectrum, and understanding of the underlying physics often requires the measurement of the broadband spectral behavior. For a bandpass stretching from 2 keV to 200 keV, W- and Pt-based coatings will suffer from the presence of the K-edge in the middle of the bandpass. As shown in Figure 3, Ni and Co do not have this restriction, but being lighter elements, they are not as efficient as either W and Pt below the Pt and W K-edge, which has limited the attention and development they have received. Some promising work, though, has been done, and a Ni/C coating has been measured up to 125 keV,[17] demonstrating good performance at these energies. However, because Ni is ferromagnetic, pure Ni films are more difficult to deposit and Ni/Si, NiV/Si, and NiV/C are more likely candidates. These have been characterized at low energies and proven to be stable, but have not been measured at energies above 80 keV.[15,18] CoCr/C coatings have been investigated by Windt (2015),[19] and significant progress was made on improving interface quality through optimization of deposition conditions; X-ray performance is still below expectations, however, and further research is thus needed to improve interface quality in both Ni- and Co-based coatings. WC/SiC is a very attractive material combination because of its very low surface roughness (< 0.3 nm) and ability to be deposited in very thin layers (< 2 nm). Coatings with up to 300 bi-layers have been measured at 300-600 keV and show good agreement with the expected performance, which makes it favorable for γ-ray reflectors.[20–22]

For the baseline design presented here, we decided to investigate the theoretical performance of Ni/C, NiV/C, and WC/SiC.

3.3 Optimizations

We employed the optimization routine used for *NuSTAR*, described in detail in,[9] and imposed the following material constraints:

Ni: 1. Maximum layer thickness 3 microns
2. Minimum thickness = 3.5 nm
3. Interfacial roughness = 0.45 nm
4. Maximum number of bilayers = 600

W: 1. Minimum thickness: 2.5 nm
2. Interfacial roughness : 0.35 nm

WC: 1. Minimum thickness: 1.5 nm
2. Interfacial Roughness: 0.3 nm
3. Maximum number of bilayers = 500

We optimized over the minimum and maximum d-spacing of the bi-layers, the relative thickness of high- and low-Z, Γ, the power-law index of the depth-profile, c, and the number of bi-layers. The typical values for Ni/C are for the minimum bi-layer thickness $d_{\rm min}$=3.5 nm (as thin as feasible), $d_{\rm max} = 5 - 19$ nm maximum thickness, $c = 0.2 - 0.3$, $\Gamma = 0.3 - 0.38$, and the number of bi-layers maxed out at 600. For NiV/C we did two optimizations where we restricted the total thickness of the stack to 1μm and 3μm, and the difference in parameters are not very different, $d_{\rm min}$=3.5 nm, $d_{\rm max} = 14 - 19$ nm, $\Gamma = 0.35 - 0.4$, $c = 0.23 - 0.28$, except for the number of bi-layers, which were 300 for 1μm and 1000 for 3μm. WC/SiC has values $d_{\rm min}$=1.5 nm, $d_{\rm max} = 10 - 14$ nm, $\Gamma = 0.35 - 0.45$, $c = 0.35 - 0.41$.

4. RESULTS AND FUTURE DEVELOPMENT

Figure 4 shows the effective area of the optimizations. All effective areas are shown without the detector response or attenuation from windows and thermal blankets folded in. We keep as reference the combined area of the two *NuSTAR* optics, and also show the effective area obtained if the *NuSTAR* recipes are applied to the *HEX-P* geometry. All *HEX-P* areas are for three modules assuming the baseline design. These optimizations show that unless NiV/C can be coated in very thick stacks, it is probably not a viable option. WC/SiC displays the best performance when considering the change of area as a function of energy, and if not for its prominent K-edge would have been the best choice. Ni/C is theoretically very promising, but as discussed above pure Ni films are difficult to deposit.

The results are thus far have not yet closed the design, and we are continuing our investigations. The main problem is the overall thicknesses of the resulting stacks, which if too thick causes the stresses between layers to degrade the interfacial roughness and reduce the reflectivity, and possibly perturb the substrate that could lead to a degradation of the angular resolution as well. From a theoretical point of view, we will continue searching the phase space for different multilayer recipes and alternatives to the power-law depth-graded profile. Perturbations to the power-law graded profile, where for example every bi-layer is tuned individually to achieve a desired target response, have typically been targeted for narrowband applications,[19,23,24] but have shown promise for broadband use as well,[25] and may be a way to overcome the problem of thick bi-layer stacks.

From a material development point of view, it is clear that we first need to establish the feasibility of Ni- and Co-based coatings above 80 keV, and determine the material constraints of minimum thickness, maximum stack thickness, and interfacial roughness to narrow down the design space. Research is also underway in the deposition methods, moving from non-reactive to reactive sputtering which has shown to reduce coating stress and decrease the interfacial roughness between layers.

Another avenue of development is hybrid coatings in which two different material combinations are joined to mitigate the impact of absorption edges, as for example from Pt and W. A hybrid coating like this was produced by Jensen et al. (2006),[15] who combined NiV/SiC and WC/SiC together in a linear graded multilayer stack of 100[NiV/SiC]/70[WC/SiC]/Si, with the NiV/SiC at the top for the low energies and WC/SiC at the bottom for the hard energies, and showed that the measured reflectivity matched the theoretical prediction for the stack design. Such hybrid coatings have yet to be measured at high energies, but the low energy performances are promising for their high energy application.

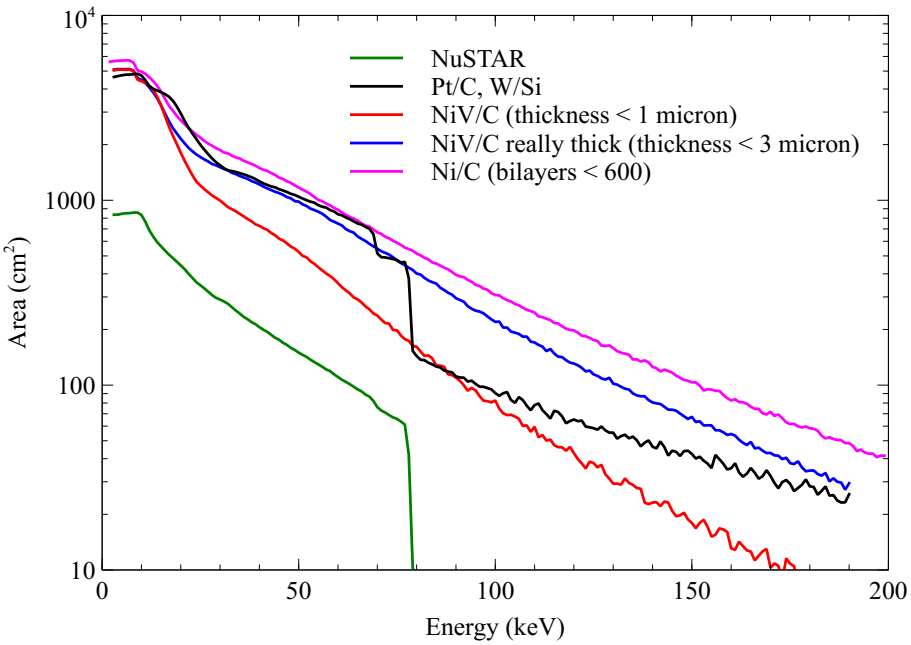

Figure 4. Effective areas of 3 modules for *HEX-P*and 2 modules for *NuSTAR*, shown without the detector response or attenuation from windows and/or thermal blankets folded in.

4.1 Alternate Designs

Generating more area is generally a matter of increasing the radius of the optics and/or adding modules, but both come at the cost of more mass. The relative ratio of low to high area can, however, be shifted without necessarily an increase in mass. This can be done by adding more modules, but reducing their overall size. Shown in Figure 5 is one such example, where the outer radius has been reduced from 350 mm to 200 mm, and instead of three modules we use six modules. The low energy suppression is due to the loss of the outer diameters shells, which are major contributors to the low energy area. Conversely, emphasis on the low energy area can be achieved by reducing the number of modules, but increasing the size of each optic.

5. SUMMARY

We have established the geometry of the *HEX-P* telescope and investigated alternative designs around the baseline, identifying as possible trades the length of the mirror shells, the size of overall optics, and the number of modules. We have run initial optimizations on multilayer coatings for the material pairs Ni/C, NiV/C, and WC/SiC, and concluded that as of yet there is no clear favorite. We plan to continue our investigations theoretically by optimizing a combination of hybrid coatings with different depth-graded profiles. We will use those results to indicate the direction of laboratory experimentation, which presently should be focused on the feasibility of Ni- and Co-based coatings above 80 keV.

REFERENCES

[1] Harrison, F. A., Craig, W. W., Christensen, F. E., Hailey, C. J., Zhang, W. W., Boggs, S. E., Stern, D., Cook, W. R., Forster, K., Giommi, P., Grefenstette, B. W., Kim, Y., Kitaguchi, T., Koglin, J. E., Madsen, K. K., Mao, P. H., Miyasaka, H., Mori, K., Perri, M., Pivovaroff, M. J., Puccetti, S., Rana, V. R., Westergaard, N. J., Willis, J., Zoglauer, A., An, H., Bachetti, M., Barrière, N. M., Bellm, E. C., Bhalerao, V., Brejnholt, N. F., Fuerst, F., Liebe, C. C., Markwardt, C. B., Nynka, M., Vogel, J. K., Walton, D. J., Wik, D. R., Alexander, D. M., Cominsky, L. R., Hornschemeier, A. E., Hornstrup, A., Kaspi, V. M., Madejski,

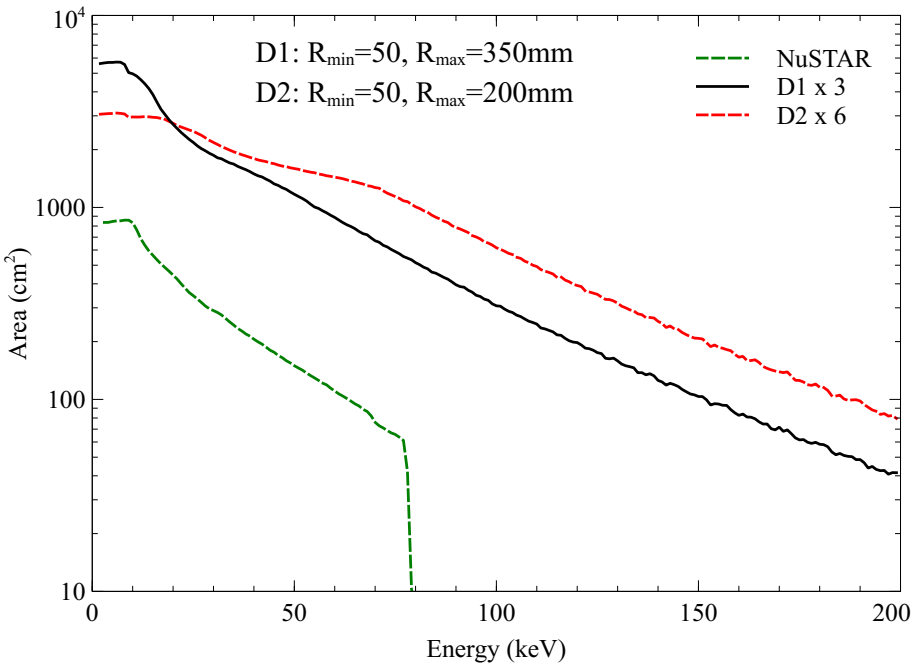

Figure 5. Trade between using 6 smaller optics (D2) and 3 larger optics (D1).

G. M., Matt, G., Molendi, S., Smith, D. M., Tomsick, J. A., Ajello, M., Ballantyne, D. R., Baloković, M., Barret, D., Bauer, F. E., Blandford, R. D., Brandt, W. N., Brenneman, L. W., Chiang, J., Chakrabarty, D., Chenevez, J., Comastri, A., Dufour, F., Elvis, M., Fabian, A. C., Farrah, D., Fryer, C. L., Gotthelf, E. V., Grindlay, J. E., Helfand, D. J., Krivonos, R., Meier, D. L., Miller, J. M., Natalucci, L., Ogle, P., Ofek, E. O., Ptak, A., Reynolds, S. P., Rigby, J. R., Tagliaferri, G., Thorsett, S. E., Treister, E., and Urry, C. M., "The Nuclear Spectroscopic Telescope Array (NuSTAR) High-energy X-Ray Mission," *ApJ* **770**, 103 (June 2013).

[2] Zhang, W. W., Allgood, K. D., Biskach, M. P., Chan, K.-W., Hlinka, M., Kearney, J. D., Mazzarella, J. R., McClelland, R. S., Numata, A., Olsen, L. G., Riveros, R. E., Saha, T. T., and Solly, P. M., "Monocrystalline silicon and the meta-shell approach to building x-ray astronomical optics," *Proc.SPIE* **10399**, 10399 – 10399 – 9 (2017).

[3] Spiga, D., Cotroneo, V., Basso, S., and Conconi, P., "Analytical computation of the off-axis effective area of grazing incidence X-ray mirrors," *Astronomy and Astrophysics* **505**, 373–384 (Oct. 2009).

[4] Spiga, D., "Optics for X-ray telescopes: analytical treatment of the off-axis effective area of mirrors in optical modules," *Astronomy and Astrophysics* **529**, A18 (May 2011).

[5] Spiga, D., "X-ray mirror module analytical design from field of view requirement and stray light tolerances," in [*Space Telescopes and Instrumentation 2016: Ultraviolet to Gamma Ray*], *Proc. SPIE* **9905** (July 2016).

[6] Madsen, K. K., Christensen, F. E., Craig, W. W., Forster, K. W., Grefenstette, B. W., Harrison, F. A., Miyasaka, H., and Rana, V., "Observational artifacts of nuclear spectroscopic telescope array: ghost rays and stray light," *Journal of Astronomical Telescopes, Instruments, and Systems* **3**, 3 – 3 – 13 (2017).

[7] Joensen, K. and et al *Appl Opt.* **34**, 7935 (1995).

[8] Madsen, K. K., Christensen, F. E., Jensen, C. P., Ziegler, E., Craig, W. W., Gunderson, K. S., Koglin, J. E., and Pedersen, K., "X-ray study of W/Si multilayers for the HEFT hard x-ray telescope," in [*Optics for EUV, X-Ray, and Gamma-Ray Astronomy*], Citterio, O. and O'Dell, S. L., eds., *Proc. SPIE* **5168**, 41–52 (Feb. 2004).

[9] Madsen, K. K., Harrison, F. A., Mao, P. H., Christensen, F. E., Jensen, C. P., Brejnholt, N., Koglin, J., and Pivovaroff, M. J., "Optimizations of Pt/SiC and W/Si multilayers for the Nuclear Spectroscopic Telescope Array," in [*Optics for EUV, X-Ray, and Gamma-Ray Astronomy IV*], *Proc. SPIE* **7437** (Aug. 2009).

[10] Tueller, J., Krimm, H. A., Okajima, T., Barthelmy, S. D., Owens, S. M., Serlemitsos, P. J., Soong, Y., Chan, K.-W., Ogasaka, Y., Shibata, R., Tamura, K., Furuzawa, A., Tawara, Y., Kunieda, H., and Yamashita, K., "InFOCμS Hard X-ray Imaging Telescope," *Experimental Astronomy* **20**, 121–129 (Dec. 2005).

[11] Takahashi, T., Kokubun, M., Mitsuda, K., Kelley, R., Ohashi, T., Aharonian, F., Akamatsu, H., Akimoto, F., Allen, S., Anabuki, N., and et al., "The ASTRO-H (Hitomi) x-ray astronomy satellite," in [*Space Telescopes and Instrumentation 2016: Ultraviolet to Gamma Ray*], *Proc.SPIE* **9905** (July 2016).

[12] Windt, D. L., Christensen, F. E., Craig, W. W., Hailey, C. J., Harrison, F. A., Jimenez-Garate, M. A., Kalyanaraman, R., and Mao, P. H., "X-ray multilayer coatings for use at energies above 100 kev," *Proc.SPIE* **4012** (2000).

[13] Windt, D. L., Donguy, S., Hailey, C. J., Koglin, J., Honkimaki, V., Ziegler, E., Christensen, F. E., Chen, C. M. H., Harrison, F. A., and Craig, W. W., "W/sic x-ray multilayers optimized for use above 100 kev," *Proc.SPIE* **4851** (2003).

[14] Christensen, F. E., Jensen, C. P., Madsen, K. K., Pivovaroff, M. J., Chen, H., Dariel, A., and Hghj, P., "Novel multilayer designs for future hard x-ray missions," *Proc.SPIE* **6266** (2006).

[15] Jensen, C. P., Madsen, K. K., and Christensen, F. E., "Investigation of new material combinations for hard x-ray telescope designs," *Proc.SPIE* **6266** (2006).

[16] Windt, D. L., "Advancements in hard x-ray multilayers for x-ray astronomy," *Proc. SPIE* **9603** (2015).

[17] Joensen, K. D., Hoghoj, P., Christensen, F. E., Gorenstein, P., Susini, J., Ziegler, E., Freund, A. K., and Wood, J. L., "Multilayered supermirror structures for hard x-ray synchrotron and astrophysics instrumentation," *Proc. SPIE* **2011** (1994).

[18] Girou, D. A., Massahi, S., Sleire, E. K., Jakobsen, A. C., and Christensen, F. E., "Development of ni-based multilayers for future focusing soft gamma ray telescopes," *Proc.SPIE* **9603** (2015).

[19] Windt, D. L. and Gullikson, E. M., "Pd/B_4C/Y multilayer coatings for extreme ultraviolet applications near 10 nm wavelength," *Applied Optics* **54**, 5850 (June 2015).

[20] Fernández-Perea, M., Descalle, M.-A., Soufli, R., Ziock, K. P., Alameda, J., Baker, S. L., McCarville, T. J., Honkimäki, V., Ziegler, E., Jakobsen, A. C., Christensen, F. E., and Pivovaroff, M. J., "Physics of reflective optics for the soft gamma-ray photon energy range," *Phys. Rev. Lett.* **111**, 027404 (Jul 2013).

[21] Brejnholt, N. F., Soufli, R., Descalle, M.-A., Fernández-Perea, M., Christensen, F. E., Jakobsen, A. C., Honkimäki, V., and Pivovaroff, M. J., "Demonstration of multilayer reflective optics at photon energies above 0.6 mev," *Opt. Express* **22**, 15364–15369 (Jun 2014).

[22] Ruz, J., Descalle, M. A., Alameda, J. B., Brejnholt, N. F., Chichester, D. L., Decker, T. A., Fernandez-Perea, M., Hill, R. M., Kisner, R. A., Melin, A. M., Patton, B. W., Soufli, R., Trellue, H., Watson, S. M., Ziock, K. P., and Pivovaroff, M. J., "Characterization and simulation of soft gamma-ray mirrors for their use with spent fuel rods at reprocessing facilities," *Appl. Opt.* **55**, 4285–4292 (Jun 2016).

[23] Morawe, C., Ziegler, E., Peffen, J.-C., and Kozhevnikov, I. V., "Design and fabrication of depth-graded X-ray multilayers," *Nuclear Instruments and Methods in Physics Research A* **493**, 189–198 (Nov. 2002).

[24] Aquila, A. L., Salmassi, F., Dollar, F., Liu, Y., and Gullikson, E., "Developments in realistic design for aperiodic Mo/Si multilayer mirrors," *Optics Express* **14**, 10073–10078 (Oct. 2006).

[25] Yao, Y., Kunieda, H., Matsumoto, H., Tamura, K., and Miyata, Y., "Design and fabrication of a supermirror with smooth and broad response for hard x-ray telescopes," *Appl. Opt.* **52**, 6824–6833 (Sep 2013).